HHS Public Access

Author manuscript

Adv Cancer Biol Metastasis. Author manuscript; available in PMC 2023 August 17.

Published in final edited form as:

Adv Cancer Biol Metastasis. 2023 July ; 7: . doi:10.1016/j.adcanc.2022.100080.

Benzophenone-3 exposure alters composition of tumor infiltrating immune cells and increases lung seeding of 4T1 breast cancer cells

Stephanie M. Morin[a,b], **Kelly J. Gregory**[a], **Brenda Medeiros**[c], **Tigist Terefe**[a], **Reyhane Hoshyar**[d], **Ahmed Alhusseiny**[e], **Shiuan Chen**[f], **Richard C. Schwartz**[d], **D. Joseph Jerry**[b], **Laura N. Vandenberg**[c], **Sallie S. Schneider**[a,b,g,*]

[a]Pioneer Valley Life Sciences Institute, Springfield, MA, 01199, USA

[b]Dept of Veterinary and Animal Sciences, University of Massachusetts, Amherst, MA, 01003, USA

[c]Department of Environmental Health Sciences, School of Public Health and Health Sciences, University of Massachusetts, Amherst, 01003, USA

[d]Breast Cancer and the Environment Research Program, Department of Microbiology and Molecular Genetics, Michigan State University, East Lansing, MI, USA

[e]University of Massachusetts Chan Medical School-Baystate, Department of Pathology, Springfield, MA, 01199, USA

[f]Department of Cancer Biology and Molecular Medicine, Beckman Research Institute of City of Hope, Duarte, CA, USA

[g]University of Massachusetts Chan Medical School-Baystate, Department of Surgery, Springfield, MA, 01199, USA

Abstract

Environmental chemicals are a persistent and pervasive part of everyday life. A subset of environmental chemicals are xenoestrogens, compounds that bind to the estrogen receptor (ER) and drive estrogen-related processes. One such chemical, benzophenone-3 (BP3), is a common chemical in sunscreen. It is a potent UV protectant but also is quickly absorbed through the skin. While it has been approved by the FDA, there is a renewed interest in the safety of BP3, particularly in relation to breast cancer. The focus of this study was to examine the impact that BP3 has on triple negative breast cancer (TNBC) through alterations to cells in the immune microenvironment. In this study, we exposed female mice to one of two doses of BP3 before

*Corresponding author. Pioneer Valley Life Sciences Institute, Springfield, MA, 01199, USA. Sallie.Schneider@baystatehealth.org (S.S. Schneider).

Declaration of competing interest

The authors declare that they have no known competing financial interests or personal relationships that could have appeared to influence the work reported in this paper.

Appendix A. Supplementary data

Supplementary data to this article can be found online at https://doi.org/10.1016/j.adcanc.2022.100080.

injecting them with a TNBC cell line. Several immune endpoints were examined both in the primary tissues and from *in vitro* studies of T cell behavior. Our studies revealed that in the lung tumor microenvironment, exposure to BP3 not only increased the number of metastases, but also the total area of tumor coverage. We also found that BP3 caused alterations in immune populations in a tissue-dependent manner, particularly in T cells. Taken together, our data suggest that while BP3 may not directly affect the proliferation of TNBC, growth and metastasis of TNBC-derived tumors can be altered by BP3 exposures via the alterations in the immune populations of the tumor microenvironment.

1. Introduction

Among American women, breast cancer is the most commonly diagnosed cancer, and it is expected that in 2022, there will be approximately 281,550 new cases of invasive breast cancer (Breastcancer.org). Only a small portion of diagnosed breast cancers are linked to heritable factors, suggesting that there are other factors, possibly environmental, that contribute to cancer development and progression [1]. It has been well documented that higher levels of estrogen in the blood are linked to elevated breast cancer risk [1,2]. Estrogens can act directly on the breast via endocrine responsive ductal epithelium of the mammary tissue, or they can act indirectly via estrogen-responsive stromal cells, which in turn release growth factors, cytokines, and reactive oxygen species to impact or damage breast epithelial cells [3,4].

Numerous chemicals utilized in everyday products fall into a category termed endocrine disrupting chemicals (EDC) [5,6]. EDCs alter one or more hormone actions including many that act as hormone receptor agonists or antagonists [7]. Since the endocrine system is responsible for the function and coordination of many organs and other systems of the body including those responsible for metabolism, reproduction, bone health, stress responses, and the immune system [1,8]; the health impacts of these chemicals are a critical area of study. Several studies have demonstrated a link between exposure to EDCs and breast cancer risk [9–12]. For example, Bisphenol A (BPA) is a well-known example of a prevalent environmental EDC which has been shown to induce estrogenic effects on various cell types, including breast epithelial cells *in vitro* and *in vivo* [13].

Benzophenone-3 (BP3) is another EDC that has well-documented ubiquitous exposures in human populations [14]. BP3 is a potent UV filter that easily absorbs into the skin and dries without visible residue, which makes it a favored chemical in many sunscreens, cosmetics, and lip balms [15–18]. While the FDA approved BP3 for use in the early 1980s, a study by Matta et al. (2019) demonstrated that daily application of sunscreen, of which the allowable maximum content of BP3 is 6% by weight, to 75% of the body resulted in blood levels of BP3 that were significantly higher than the level deemed safe [19]. BP3 is also found in numerous other consumer products including fabrics, paints, and food packaging materials which all likely contribute to daily human exposures [20]. 97% of women had detectable levels of BP3 in their urine [21], demonstrating that it is a pervasive chemical. BP3 may react with other chemicals in the environment as well. For example, BP3 is reactive with chlorine and has been shown to produce a “hazardous” by-product that is able

to concentrate in swimming pools and wastewater treatment plants [22,23]. Coral reefs are biologically diverse and productive ecosystems which appear to be at particular risk for the effects of BP3. In a laboratory setting, high concentrations of BP3 in the water have been shown to be toxic to coral and are suspected to contribute to coral bleaching [23–25]. In animals, exposure to BP3 was able to alter the morphology of the mammary gland of parous mice, and the offspring of those dams also exhibited morphological changes to the mammary gland in adulthood [26,27]. Taken together these studies suggest that the impact of BP3 warrants further scrutiny due to the potential effects it may have on human and environmental health [9,24,25,28–32].

BP3 has weak agonistic effects on estrogen receptor positive (ER+) breast cancer cells through direct interaction with the ER or through modulation of enzymes responsible for the synthesis of estrogen [33,34]. However, the impact of BP3 on triple negative breast cancer has not yet been investigated because these cells do not express the ER. This is an overly reductionist view since many of the immune cells in the surrounding tumor microenvironment express hormone receptors, and modulation of these receptors can impact the behavior of these non-epithelial cell types. In particular, the immune compartment of the tumor microenvironment is known to be affected by estrogens. T lymphocytes express both nuclear ER isoforms (ERα and ERβ) [35]. These immune cells are a subset of the adaptive immune system that exhibit relative plasticity and can be polarized into several phenotypes, including but not limited to T helper cells, T regulatory cells, and cytotoxic T cells. Th2-polarized T lymphocytes release cytokines, including IL-4 and IL-13, and are required for mounting the response to extracellular pathogens and allergic responses [36,37]. Cytokines released from T cells act in an autocrine fashion to regulate their expansion and in a paracrine fashion to alter the behavior of macrophages toward a wound healing and anti-inflammatory M2 phenotype. Th2 cells express chemokine receptors, including CCR3, CCR4, and CCR8 to help them migrate toward sites of pathogen infection [38]. Th1-polarized T lymphocytes, on the other hand, secrete IFNγ, IL-2, and TNFα to expand cytotoxic T cell subsets and express the chemokine receptors CCR5 and CXCR3, which facilitate their migration toward sites of inflammation [39,40]. The balance between the T helper subsets and their impact on the expansion of other T cell subsets (cytotoxic T cells, Th17, and Th22) can contribute to differences in cancer susceptibility and progression [41,42]. Interestingly, exposure to estrogen modulates the levels of cytokine expression in $CD4^+$ T helper lymphocytes, shifting them away from the Th1 response toward a more Th2-like response [43, 44]. The leading population of cells involved in the suppression of T cell activity are T regulatory (Treg) cells which are affected by the presence of estrogens. Specifically, estrogen can cause a rapid expansion of $Foxp3^+CD25^+$ Treg cells [45–47].

In this study, we investigated whether BP3 could alter the behavior of an ERα negative breast cancer cell line *in vitro,* as well as *in vivo,* where the tumor cells are surrounded by complex cell types, many of which express hormone receptors. We found that while primary tumor growth was not altered following BP3 exposure, the chemical did significantly impact the ability of 4T1 cells to establish metastases in the lung. This difference in lung metastatic involvement was associated with a decrease in infiltrating T cell populations and an increase in eosinophils within the lung lesions. Chemokine expression, which is important for cell trafficking, was also impacted by BP3 exposure in a tumor and tissue-specific fashion. *Ex*

vivo studies highlighted that exposure to BP3 decreased the activation-induced proliferation and cytokine secretion of $CD4^{+}$T cells. The Treg phenotype was also destabilized by this exposure. Taken together these data reveal the potential for increased risk of breast cancer metastasis in women exposed to BP3.

2. Methods

2.1. Animals

This study was carried out in strict accordance with the recommendations in the Guide for the Care and Use of Laboratory Animals of the National Institutes of Health. The protocol was approved by the Baystate Medical Center Institutional Animal Care and Use Committee (Permit Number: 1331754-4). 3-week-old BALB/c female mice were fed control chow (n = 20), or chow intended to deliver 3 mg/kg body weight/day BP3 (n = 20), or 70 mg/kg body weight/day BP3 (n = 20). BP3 was compounded into the rodent chow (10% kcal fat; D11012202; Research Diets, New Brunswick NJ). 2- hydroxy-4-methoxybenzophenone (BP3) was obtained from Sigma -Aldrich (#H36206). Mice were fed their assigned chow *ad libitum* from weaning through puberty to the end of the experiment. At 8 weeks of age, the animals were injected with the ER negative murine breast cancer line, 4T1, either intra-mammary into the 4th inguinal mammary fat pad (n = 10/treatment), or intravenously via the tail vein (n = 10/treatment). 4 × 10 [5] cells/100 μL were injected into each mouse. At 3 weeks post-injection, the intramammary injected mice were euthanized; at 2 weeks post-injection, the intravenously injected mice were euthanized. Mammary glands, primary tumors, intestines, spleens, and lungs were extracted from each mouse and snap frozen for later RNA extraction or fixed in 10% buffered formalin for histological analysis.

2.2. Immunohistochemistry

Tissues were fixed in 10% buffered formalin for 24 h at 4 °C, after which the tissues were moved to 70% ethanol for at least 24 h before processing. Tissues were processed in a Leica ASP300S processor before being embedded in paraffin. Tissue blocks were sectioned at a thickness of 4 μm and mounted on charged slides. Sections were deparaffinized in xylenes, rehydrated in ethanol, and rinsed in phosphate buffered saline (PBS). Immunohistochemistry (IHC) was performed on a DakoCytomation autostainer, using the envision HRP Detection system (Dako, Carpinteria, CA). Antigen retrieval was performed in a microwave at 98 °C in 0.01 M citrate buffer. After cooling for 20 min, sections were rinsed in TBS and incubated with primary monoclonal antibodies (Table 1) for 30 min. After a subsequent wash in TBS, slides were incubated with corresponding secondary antibody (Table 1) for 20 min. Immunoreactivity was visualized by incubation with the chromogen diaminobenzidine (DAB) for 5 min. Tissue sections were counterstained with hematoxylin, dehydrated through graded ethanol and xylenes, and then cover slips were applied. Images were captured with an Olympus BX41 light microscope using SPOT Software 5.1 (SPOT™ Imaging Solutions, Detroit, MI) [48].

2.3. Eosinophil staining

For identification of eosinophils, deparaffinized 4 μm sections were stained with Vital New Red [49]. Sections were visualized using a Nikon Eclipse 400 microscope and a SPOT

RT color camera with SPOT software (Diagnostic Instruments, Sterling Heights, MI). The number of eosinophils is expressed as cells per 40X visual field within tissue sections. For each sample, between 3 and 9 visual fields were quantitated.

2.4. MTS proliferation assay

4T1 cells were plated at a density of 1 × 10 [4] cells/well in a 96-well plate. Twenty-four hours later, the cells were exposed to BP3 treatment for 72 h. CellTiter 96 Aqueous One Solution MTS (Promega, Madison, WI) was used according to manufacturer's instructions to detect alterations in the number of viable cells. The absorbance of each well was measured at 490 nm wavelength using an Enspire® multimode automated plate reader (PerkinElmer, Waltham, MA) [50].

2.5. Scratch wound

4T1 cells were seeded in 6 well plates and grown until they reached 80% confluence. Cells were treated with 30 μM BP3 or vehicle for 24 h, at which time a wound was made in the cell layer with a pipette tip. Images were taken at 0 h, 24 h, and 48 h. Closure of the wound was measured using ImageJ.

2.6. Transwell assay

4T1 cells were plated at a density of 5 × 10 [5] cells/well in a Transwell plate (Corning, Corning, NY) and were exposed to 30 μM BP3 for 24 h. For chamber assays, 4T1 cells were grown to 70% confluence and pre-treated with either 0.1% DMSO or 30 μM BP3 for 2 weeks. The pretreated cells were trypsinized, centrifuged at 1000×*g* for 4 min, and brought to a concentration of 4.3 × 10 [5] cells/mL in serum-free media in Transwell permeable supports (Corning) above media containing 10% FBS. Following a 24-h incubation, Transwells were removed and fixed in 10% formalin for 10 min, stained with 10% Crystal Violet for 10 min, and rinsed with dH_2O. Cells that did not migrate were removed from the upper surface by scrubbing with 1X PBS moistened cotton-tipped swab. The insert was removed from the chamber with a scalpel and mounted on a microscope slide with Cytoseal™XYL mounting media (Thermo Fisher Scientific, Waltham, MA). Images were captured with an Olympus BX41 light microscope using SPOT Software 5.1 (SPOT™ Imaging Solutions).

2.7. RNA isolation and real-time PCR analysis

Total RNA was extracted from T cells and whole organs by lysis in Trizol (Invitrogen Waltham, MA) according to the manufacturer's instructions. Whole organs were further processed using the Direct-zol RNA Kit (ZYMO Research, Irvine, CA) to further purify the RNA. Relative expression levels of mRNA were determined by quantitative real-time PCR (qRT-RCR) using the Mx3005P® real-time PCR system (Agilent, Santa Clara, CA) and all values were normalized to the amplification of β-actin (ACTB). The PCR primer sequences for human ACTB have been published previously [51] while other primer sequences were designed to cross exon junctions using NCBI primer-blast and are described in Table 2. The assays were performed using the 1-Step Brilliant® SYBRIII® Green qRT-PCR Master Mix Kit (Agilent) containing 200 nM forward primer, 200 nM reverse primer, and 20 ng total

RNA. The conditions for cDNA synthesis and target mRNA amplification were performed as follows: 1 cycle of 50 °C for 30 min; 1 cycle of 95 °C for 10 min; and 35 cycles each of 95 °C for 30 s, 55 °C for 1 min, and 72 °C for 30 s. Non-template controls and reverse-transcriptase absent controls were included to control for primer dimers and for genomic DNA amplification, respectively [52].

2.8. Protein analysis

To evaluate secreted protein levels from immune cells, supernatants were collected at the time of RNA isolation. Using the V-Plex, Proinflammatory Panel 1 (mouse) Kit (Catalog # K15048D) from Meso Scale Discovery (Rockville, MD), cytokine levels were measured according to manufacturer's standards. Chemokines were analyzed using mouse CCL2 ELISA kit (#88-7391-22, Invitrogen), mouse MIP-1alpha (CCL3) ELISA kit (#88-56013-22, Invitrogen), and the TGFβ ELISA kit (#88-8350-00, Invitrogen) according to the manufacturer's instructions.

2.9. Bone marrow derived macrophage (BMDM) cell culture

Femurs were harvested from BALB/c female mice, and bone marrow was harvested from the bone shaft through flushing with HBSS until the bone appeared pale white. Cells were treated with ACK buffer (NH_4Cl, $KHCO_3$, EDTA disodium) for 5 min at RT to lyse the red blood cells. Cells were spun down at 300×*g* for 5 min, the supernatant was removed, and cells were resuspended in DMEM media (Thermo Fisher Scientific), 10% FBS (Sigma-Aldrich, St. Louis, MO), 2-mercaptoethanol (Sigma-Aldrich), antibiotic/antimycotic (Thermo Fisher Scientific) before being passed over a 100 μm filter. Cells were plated in a 24-well plate at a density of 1 × 10 [6] cells/well in media containing 25 ng/mL MCSF (Stemcell Technologies, Vancouver, Canada). Cells were incubated at 37 °C with 5% CO_2 for a minimum of 7 days replacing half of the volume of media every 3 days.

After 7 days, BMDM media was removed and conditioned media from 4T1 cells or 3T3 cells was used at a 1:1 ratio with BMDM native media. Conditioned media was made by using native media for the cell line and leaving on the cells for 24 h, after which time the media was collected and the solids were spun out.

2.10. T cell culture

Spleens were resected from female BALB/c mice and were teased apart in PBS to release splenocytes. Cells were then treated with red blood cell lysis buffer (Sigma-Aldrich) according to manufacturer's standards for 10 min at room temperature. $CD4^+$ T cells or pan naïve T cells were isolated using negative selection kits according to manufacturer's specifications (Invitrogen). Isolated T cells were cultured on plates coated with 3 μM/mL anti-CD3 (Invitrogen #16003185) and cultured in RPMI (Gibco) supplemented with 10% FBS (Sigma-Aldrich). recombinant IL-2 (10 ng/mL) (R&D Systems Catalog # 402-mL) and anti-CD28 (1:75 dilution of 1 μg/mL) (Invitrogen #16028182). Cells were cultured for 48 h and then cell number and viability were measured, conditioned media was collected, and the cells were put in Trizol for RNA isolation.

To polarize toward T regulatory (Treg) cells, cells were cultured and activated as above, but the media was supplemented with retinoic acid (RA) (2 μg/mL) (Sigma-Aldrich) and TGF-β (20 ng/mL) (Abcam Ref# ab50036) for 96 h (adapted from Ozay et al., 2020) [53] before being stained for flow cytometry or put in Trizol for RNA isolation.

2.11. Conditioned media

To make conditioned media, immortal cell lines were grown to 80% confluence in the corresponding media. Cells were then trypsinized and plated in 10 cm plates at a concentration of 2 × 10 [6] cells and left to adhere for 24 h. Cells were then treated with 30 μM BP3 or DMSO and left for 48 h at which time the media was removed, solids were spun out and the media was aliquoted and stored at −20 °C until use.

Primary immune cell lines were cultured as previously described. Cells were grown in 24 well plates and fresh media was added ± 30 μM BP3 and cultured for 48 h before being collected, spun down and stored for later use. T regulatory cells were cultured as previously described for 96 h before conditioned media was collected.

2.12. Flow cytometry

T regs were cultured as described for 96 h, gently dissociated from the plate, and spun down at 5000 RPM for 10 min. Conditioned media was removed and saved for later use. Cells were fixed and permeabilized with the eBioscience FoxP3 fixation/permeabilization kit (Thermo Fisher Scientific #00-5521-00) according to manufacturer's protocol. Cells were then taken up in flow buffer (1X PBS and 0.1% BSA), and stained with Foxp3 (Abcam Cat# ab218773), CD4 (AbCam Cat #ab269349), and CD25 (AbCam Cat# ab210330) for at least 30 min on ice protected from light. Cells were spun down; the supernatant was removed, and cells were washed in flow buffer once before being resuspended in 100 μL flow buffer. Flow cytometry was run on the Amnis FlowSight imaging flow cytometer and analysis was performed using IDEAS 6.2 software.

2.13. Statistics

Graphpad Prism was used to compare group means using Student's t-tests and results with $P < 0.05$ were considered significant.

3. Results

3.1. BP3 does not alter primary tumor growth, but does increase lung metastatic lesions

Many studies examining the impact of xenoestrogens on cancer growth focus on ER + breast cancer cell lines since proliferation of many mammary epithelial cells is driven by estrogen. However, the overall goal of this study was to establish whether BP3 could contribute to breast cancer growth or progression through its effects on immune cells of the tumor microenvironment. Therefore, we chose to study a breast cancer line which would not be directly affected by a xenoestrogen. 4T1 cells are a murine triple negative breast cancer (TNBC) cell line that do not express ERα. To first determine whether BP3 could affect breast cancer cell proliferation or migration via an ER independent pathway, 4T1 cells were treated with BP3 and analyzed for viability and migration. The impact of increasing

concentrations of BP3 (0, 0.3, 3, and 30 μM) on the proliferation/viability of 4T1 cells was measured after 72 h of treatment. There was no significant difference in the number of viable cells at any of the concentrations when compared to the control (Fig. 1A). The migratory behavior of the cells was also measured via scratch wound and Transwell assays. There was no significant difference in the ability of the 4T1 cells to migrate across a scratch when treated with 30 μM BP3 (Fig. 1B). However, exposure to 30 μM BP3 reduced the ability of the cells to cross a membrane toward a chemotactic factor (Fig. 1C). This suggests that while BP3 treatment does not cause changes in the proliferation/viability or motility of the cells, it may reduce migration via an ERα independent mechanism.

To address the question of whether exposure to BP3 could affect tumor growth *in vivo*, BALB/c female mice were fed chow containing vehicle or one of two different concentrations of BP3 intended to expose the animals to doses of 3 mg/kg body weight/day or 70 mg/kg body weight/day. These dosages were chosen because it is difficult to directly compare human exposures to mice due to the differences in the metabolic rates, therefore 3 mg/kg body weight/day was chosen as it is the established NOAEL dosage [27,54], while the higher dosage (70 mg/kg body weight/day) results in urine concentrations of BP3 metabolites in mice similar to those observed in the urine of humans with heavy topical application of sunscreen [55,56]. At 8 weeks of age, following 5 weeks of BP3 exposure via chow consumption, 4T1 tumor cells were injected into the mammary fat pad (IM) to examine primary tumor growth, or intravenously via the tail vein (IV) to examine metastatic seeding and growth in the lung. Animals were euthanized at 21- or 14-days post-injection, respectively (Fig. 1D).

The weight of the mice was monitored throughout the study, and there were no significant changes in the body weights across the treatment groups in either the IM or IV mice suggesting that the inclusion of the chemical in the chow did not alter the amount of food consumed by the mice (Fig. 1E). There were no significant differences in the volume of the primary tumors across the exposure groups (Fig. 1F). However, the lungs from the IV injected mice exposed to 70 mg/kg/day BP3 exhibited significantly more tumor foci compared to lungs from the control mice (Fig. 1G), as well as significantly more tumor coverage of the lungs (Fig. 1H). To determine whether a difference in the balance of apoptosis and proliferation could explain the increased tumor coverage, lung sections were stained with antibodies to detect Caspase-3 or Ki-67 respectively. No difference in apoptotic death was noted, however, there was a decrease in the number of positively stained Ki-67 cells in the animals exposed to 70 mg/kg/day BP3 (Fig. 1I–K).

3.2. BP3 affects infiltrating immune cell populations in a tissue-dependent fashion

The impact of BP3 exposure on metastatic establishment and not primary tumor growth indicated that there was either a tissue specific impact or a change in immune cell types that alter lung establishment and not mammary gland establishment. 4T1 progression and lung seeding has been shown to be impacted by myeloid cells, such as macrophages and dendritic cells, as well as T cell subsets [57,58]. To investigate the potential impact that BP3 has on the immune populations in and around the primary tumor and lung metastatic lesions, the tissues were stained with markers for innate and adaptive immune subtypes.

Cells of the innate immune system, such as eosinophils, neutrophils, and macrophages, are the first line of defense against pathogens, but are also imperative for signaling to T and B cells to mount a more robust immune response. There was a significant increase in the number of eosinophils in the lung lesions from mice exposed to 70 mg/kg BW/day BP3 (Fig. 2A) however there was no change in the number of neutrophils (NIMP-14 stained) cells in the lung metastases (Fig. 2A). There was no significant change in the number of macrophages in the lung metastases as indicated by F4/80 staining. The majority of the F4/80^{+} cells remained toward the edge of the metastases in all groups (Supplemental Fig. 1A). The expression of CD163, a marker of immunosuppressive M2c polarized macrophages [59], was similarly localized around the edge of the lesions. However, the expression of CD206 (which can identify dendritic cells, as well as macrophages) was seen throughout the lung lesions (Supplemental Fig. 1B). Interestingly, CD25 (IL2ra) the receptor for IL2 was localized throughout the metastases similarly to the CD206 staining (Supplemental Fig. 1C). Phenotypic analysis suggested that the majority of the CD25 staining cells did not have a typical lymphocytic morphology and were likely a myeloid-related cell type (Supplemental Fig. 1C).

The adaptive immune system (B cells and T cells) has been implicated in the control of 4T1 progression [60,61]. CD45r was used to identify the B lymphocyte population in the lungs. No significant change was noted following exposure to either dose of BP3 (Fig. 2A). Antibodies specific to classical markers for cytotoxic T cells (CD8), T helper (CD4), and T regs (Foxp3) were used to stain sections of the IV lungs. In the lung metastases, exposure to 70 mg/kg BW/day BP3 resulted in a significant decrease in the expression of all T cell markers (Fig. 2B). Contrary to our hypothesis that we would observe an increase in Tregs, we detected a particularly striking decrease in Foxp3 protein staining in the lung metastases of animals treated with 70 mg/kg BW/day BP3. This appeared to be due to a dramatic drop in protein expression because enhancement and alteration of the image analysis cut-off revealed that there were lighter Foxp3 staining cells in the background (Fig. 2C). To determine whether BP3 had a systemic impact on Foxp3 expression in the mouse, we examined the lymph nodes of the mammary glands, spleen, and gut associated lymph tissue (GALT) (Supplemental Fig. 2). Interestingly, we detected no change in Foxp3 protein levels in the spleen following 70 mg/kg BW/day BP3 exposure, a decrease in Foxp3 expression in the cells of the mammary gland lymph node similar to the lung, but an increase in the number of Foxp3 staining cells in the intestinal GALT (Supplemental Fig. 2A –C).

To determine whether exposure to BP3 resulted in similar changes in immune populations (decreased T cell numbers and increased eosinophils) in the primary tumor, immunohistochemical analysis was extended to these tissues. Similar to the lung metastases, an elevation of eosinophils was noted in the primary tumors of animals treated with 70 mg/kg BW/day BP3. However, BP3 exposure had no effect on the expression of CD4 in the primary tumors. In fact, there were very few positively staining cells infiltrating within the primary tumors (Fig. 2D). There was no effect on the numbers of FoxP3 staining cells in the primary tumors, however, CD8 was significantly increased by exposure to the highest concentration of BP3 (Fig. 2D).

Taken together, these data suggest that BP3 is driving a microenvironment which supports the accumulation of eosinophils and suppresses T cell infiltration or expansion specifically within the lung tissue. Furthermore, BP3 exposure contributes to a tissue-dependent difference on either Foxp3 expression in T regs or trafficking of Treg cells to specific areas.

3.3. BP3 affects chemokine gene expression in vivo

Previous studies on endothelial cell lines have suggested that chemokines such as CCL2 (MCP1) are a critical target of BP3 (TOXNET link). Therefore, we sought to determine whether altered chemokine signaling resulted in the observed changes in immune cell trafficking. RNA was isolated from both the IV and IM lungs as well as the primary tumor from the IM injected animals and chemokine expression was examined by qRT-PCR. We observed a significant upregulation of *Ccl2* and *Ccl3(Mip1alpha*) expression in the lungs of animals exposed to 70 mg/kg BW/day BP3 (Fig. 3A). This upregulation was not seen in the lungs of mice that did not have 4T1 metastatic lesions (IM lungs) nor was it observed in the primary tumors from mice treated with 70 mg/kg BW/day BP3 which suggests that *Ccl2* and *Ccl3* chemokine upregulation is dependent upon both BP3 and crosstalk between the tumor and lung parenchyma (Fig. 3A). Interestingly, *Ccl4 (MIP1beta)* and *Ccl5 (Rantes)* were both downregulated in the lung tissue in a BP3 and tumor-dependent fashion.

CCl2 high, CCL5 low breast tumors are often associated with a Th2-like response and an increase in expression of the Th2 trafficking cytokine, *Ccl22* [62]. Therefore, we examined lungs to determine whether *Ccl22* was also elevated in response to 70 mg/kg BW/day BP3. CCL22 is often expressed by myeloid cells and is involved in the recruitment of T regulatory cells and an immunosuppressive environment [63,64]. In both the IV lungs and the primary tumors of animals exposed to 70 mg/kg BW/day BP3 there was a significant increase in the expression of *Ccl22*. There was no effect on gene expression in the IM lungs (BP3 on normal lung tissue) (Fig. 3A), which indicates that a BP3 and tumor interaction is important for the expression of this chemokine. Immunohistochemical staining of tissues with CCL22 specific antibodies demonstrated that the highest expressing cells were found in lymph nodes (Supplemental Fig. 3) consistent with its expression on myeloid/dendritic cells. Consistent with an immunosuppressive environment, the expression of indoleamine 2,3-dioxygenase (*Ido-1*) was also upregulated in the lungs of animals with 4T1 tumors and treated with BP3 regardless of tumor status (Fig. 3A). Furthermore, there was no significant change in *Ido-1* expression in the primary tumor (Fig. 3A).

Since *Ccl2* and *Ccl3* upregulation appeared to be lung- and tumor-specific, we wanted to determine which cells might be expressing the chemokines and whether a crosstalk mechanism between cells is important for their dynamic secretion. The impact of BP3 on CCL2 and CCL3 protein secretion was examined in 4T1 tumor cells, bone marrow-derived macrophages (BMDM), BMDM cultured with conditioned medium (CM) from 4T1 cells, and BMDM cultured with CM from a fibroblast line (3T3). ELISA data demonstrated that while BMDM and 4T1 alone secreted low levels of CCL2 when BMDMs were cultured with conditioned 4T1 medium, there was a significant increase in the level of CCL2 protein released from macrophages treated with CM (Fig. 3B). Exposure to BP3 significantly reduced the secreted levels of CCL2 when BMDMs were exposed to 4T1

CM. Conversely, our fibroblast cell line (3T3) secreted high levels of CCL2 without any treatment and BP3 induced a trend upwards ($p = 0.08$) in CCL2 expression (Fig. 3B). The results of the BMDMs cultured in 3T3 CM demonstrated a similar significant increase in CCL2 expression, however it is unclear whether the CCL2 was derived from the 3T3 cells themselves or was induced by 3T3 CM (Fig. 3B). Analysis of CCL3 secretion suggested a slightly different pattern, in that CCL3 was secreted at low levels from all of the cells alone, but BMDMs treated with 4T1 conditioned media or 3T3 conditioned media exhibited a significant elevation in CCL3 secretion (Fig. 3C). BP3 treatment of fibroblasts produced CM that significantly impaired CCL3 secretion from BMDMs (Fig. 3C). Taken together, these results support an impact of BP3 on CCL2 and CCL3, which is dependent on the cellular crosstalk.

3.4. BP3 affects T cell activation

Considering the observed decrease in T cell numbers and markers despite the elevated expression of chemokines in the lung tissues that are associated with increased Th2 cells, we wanted to determine if the reduction in T cells was due to an impairment in T cell expansion or in polarization of T cells. Since T cells are known to express ER and T cell activity is driven by changes in estrogen levels, we chose to examine the direct effect of BP3 exposure on activation-induced proliferation and the expression of Th1/Th2 cytokines and Treg polarization. $CD4^+$ T cells were purified from mouse spleens and the T cells were activated with anti-CD3/CD28 in the presence of IL-2. Anti-CD3/CD28 activation induced the enlargement and proliferation of the T cells along with cytokine expression (Fig. 4). However, the addition of 30 μM BP3 during T cell activation suppressed lymphoblast formation and reduced overall T cell numbers (Fig. 4A). An assessment of viability after exposure to 30 μM BP3 suggested that BP3 did not affect viability, indicating that the decrease in the number of T cells was due to reduction in T cell proliferation (Fig. 4A). RNA and supernatants were collected from the cells to determine whether BP3 altered the production of cytokines. At the RNA level, a significant reduction in *Il2* expression was noted, but there was no significant change in the mRNA levels of *Ifng* or *Il4*, which are associated with Th1 and Th2 T cell subtypes, respectively (Fig. 4B). Interestingly, analysis of protein secretion demonstrated that exposure to 30 μM BP3 caused overall decreases in cytokine secretion (Fig. 4C). We were not able to confirm the reduction of IL-2 protein levels due to its addition to the media during cell culture.

We next evaluated the expression of transcription factors associated with T cell polarization in the activated $CD4^+$ T cell population. We observed a significant increase in the expression of *Bcl6*, a transcriptional repressor that is inhibited by IL-2 [65] (Fig. 4D). However, there was no significant change in the levels of Th1 or Th2 associated transcription factors, *Tbx21* or *Gata3*, respectively [66,67] (Fig. 4D). These data indicate that *in vitro* BP3 generally suppresses T cell activation. To examine pathways that are required for T cell activation, we analyzed gene expression of metabolic markers associated with glycolysis, cell cycle, and exhaustion. Expression of *Hk2* and *Pkm*, two genes involved in the activation-induced glycolysis program, were increased as expected following T cell activation, and were not significantly affected by BP3. However, *Ldha* expression was significantly reduced following exposure to BP3. We did not observe a change in either of the T cell exhaustion

markers (*Lag3, Pdcd1*), which suggests that BP3 does not affect T cell exhaustion *in vitro*. Lastly, we found that there were no significant changes in p21 (*Cdkna1*) gene expression, which indicates that BP3 does not arrest growth or drive cells into quiescence (Fig. 4D).

3.5. BP3 suppresses the polarization of T regs in vitro

We suspected that the reduction in Foxp3 protein expression may also be the result of a decrease in T cell polarization toward this phenotype. To examine the impact of BP3 on inducible Tregs (iTregs), retinoic acid and TGF-β were included with the IL-2 and antibodies to the TCR complex when stimulating $CD4^+$ cells. A time course was performed to measure the level of $CD25^+$ and $Foxp3^+$ induction by flow cytometry as a measure of Treg cell polarization (Fig. 5A). CD4 cells were able to polarize to iTregs in the presence of 30 μM BP3, however the stability of the $CD25^{high}$ $FoxP3^{high}$ Treg phenotype was lost by 96 h post-treatment (Fig. 5A). We observed the expected increase over time in the secretion of the immunosuppressive cytokine, IL-10, but the presence of BP3 dampened that expression (Fig. 5B). Interestingly, by 96 h the impact of BP3 on IL-10 was diminished. A reduction in the expansion of Tregs was noted in the cells exposed to BP3, similar to the reduction noted in activated T cells (Fig. 5C). ELISA assays demonstrated that TGF-β secretion was upregulated when the cells were polarized toward the T reg phenotype, however BP3 dramatically reduced the secretion of the TGF-β (Fig. 5D). As expected, the secretion of both Th1-associated cytokines (IFNγ and TNFα) and Th2-associated cytokines (IL4 and IL6) were significantly reduced in polarized Tregs, however BP3 further suppressed IFNγ and TNFα (Fig. 5E). No reversal of cytokine suppression was noted in the cells exposed to BP3. We examined other Treg-associated gene expression following exposure to BP3. Upon Treg polarization (+TGFβ +RA), there was an expected decrease in the levels of *IL-2* mRNA, which was not affected by BP3 (Fig. 5F). BP3 caused no significant change in the expression of *Nrp1,* which is required for Treg stability [68], but there was an upward trend in the expression of *Ido1* (Fig. 5F). Taken together, these data suggest that a concentration of 30 μM BP3 can suppress the proliferation of Treg cells and reduce the secretion of some Treg-associated cytokines.

4. Discussion

Previous studies have shown that there are potential health risks following exposure to BP3 [69–71]. However, the majority of studies look at this endocrine disruptor in tumors that express an estrogen receptor [27,72]. The work described in this study demonstrates that exposure to 70 mg/kg BW/day BP3 in mice from 3 weeks of age onwards facilitates the seeding and growth of a triple negative breast cancer cell line in the lung but does not significantly impact the growth of primary tumors. The increase in lung metastatic coverage is associated with an increase in the number of eosinophils and a decrease in lymphocytes, particularly cytotoxic and Treg cells. Analysis of chemokines responsible for trafficking myeloid and T cell subsets demonstrated that there was a tissue and tumor specific interaction with BP3. *In vitro* studies confirmed the complex crosstalk between cell types leading to changes in the expression of chemokines CCL2 and CCL3, and also confirmed a direct effect of BP3 on the activation of iTreg cell proliferation and cytokine secretion. While epidermal exposure was not measured, there is evidence to suggest that

in humans, coverage of 75% of the body surface area in sunscreen yielded plasma levels of BP3 exceeding 0.5 ng/mL which is the threshold of toxicological concern, a concept adopted by the FDA where a substance can migrate from packaging into food. In the Matta et al. study, they found that the mean maximum plasma levels reached 258.1 ng/mL BP3 [19]. Our initial findings of alterations in the tumor metastasis and immune populations provide insight into the effects of BP3 exposure and have opened the door to further investigation as to the impacts of other routes of exposure.

Triple negative breast cancer is difficult to treat and frequently highly invasive [73]. The metastasis of this tumor type is often facilitated by stromal cells from the tumor microenvironment [74–77]. Metastatic seeding of 4T1 tumor cells is facilitated by immune cell types, such as M2 and alveolar macrophages, myeloid-derived suppressor cells and Treg cells [75,78–80]. These cells help to promote tumor cell migration, as well as a more immunosuppressive microenvironment. The tumor cells are trafficked to the tissue via expression of various chemokines interacting with specific cell surface receptors. Our results suggest that BP3 exposure alters the lung microenvironment to impact the accumulation of immune cells in the vicinity of 4T1 tumor lesions. Specifically, we demonstrate that BP3 results in increased eosinophils and decreased T lymphocytes in these lesions. Interestingly, it had been previously shown that 4T1 lung metastases exhibit a high lymphocyte to granulocyte ratio in the early stage of lung metastatic development, but over time evolves toward a very high granulocyte to lymphocyte ratio [81]. Thus, it is conceivable that BP3 exposure either accelerates this natural tumor progression in the immune landscape or alters the initial events involved in tumor formation.

Signals critical for chemotactic tissue transitions were examined in the lungs and tumors from mice exposed to BP3. Several chemokines demonstrated clear shifts in expression patterns, which could explain the alterations we observed in cell infiltration. The expression of *Ccl2, Ccl3* and *Ccl22* increased in the lungs of animals with 4T1 lesions following BP3 exposure, while *Ccl4* and *Ccl5* expression decreased in the BP3 exposed group. Interestingly, these changes were not observed in the primary tumors of BP3 exposed animals, suggesting a tissue specific interaction. Furthermore, 4T1 cells were also required for some of the observed changes suggesting both tissue and tumor interactions. This dependence upon local microenvironment is consistent with previous studies demonstrating differences in chemokine expression in 4T1 lesions [62,82]. CCL2 is a monocyte chemoattractant that can be secreted by many cell types, including tumor cells [83]. CCL2 recruits macrophages expressing CCR2 to the tumor microenvironment (TME), where the microenvironment can further alter the behavior of the macrophages, often towards phenotypes that promote tumor growth [84]. Previous studies have demonstrated that 4T1 lung metastases are associated with CCL2 expression, and cell-specific deletion experiments have indicated that CCL2 released from the stromal cells contribute to the metastatic seeding [84,85]. There are several instances of cross talk between tumor cells, macrophages and/or fibroblasts which ultimately fuel tumor progression. For example, CXCL1-induced CCL2 release from fibroblasts can promote cholesterol synthesis in 4T1 cells to encourage metastatic growth [86]. Furthermore, CCL2 crosstalk between cancer cells and fibroblasts results in increased breast cancer stem-like behaviors which can promote resistance to death [87]. Elevated CCL2 causes chemotaxis and retention of inflammatory macrophages via

secretion of CCL3 leading to enhancement of breast cancer lung metastatic involvement (Kitamura 2015) [88]. CCL3 is released from many cell types and interacts with CCR1, CCR4 and CCR5 on cell surfaces of T cells, macrophages, myeloid derived suppressor cells and eosinophils to help them move to sites of inflammation [89–91]. Previous studies have suggested that a shift in the balance towards high CCL2 and low CCL5 results in upregulation of CCL22 and an immunosuppressive tumor microenvironment [62]. CCL22 is also a chemotactic for eosinophils, particularly in the lungs, which aligns with the increase that we see in eosinophils [92,93]. This is consistent with this study where we observed an associated increase in *Ccl22* in response to BP3.

The impact of BP3 on immunosuppression is suggested not only by the reduction in tumor infiltrating T cells, but also by the increase in *Ccl22* in lymph nodes and CD25 on myeloid cells scattered throughout the lesions. Tolerogenic dendritic cells often express CD25, which is believed to act as an IL2 sink to rob T cells of a vital cytokine [94]. The increase in *Ido-1* expression provides further support for this idea. IDO-1 is a metabolizing enzyme that catalyzes the first step of the kynurenine pathway which is known to promote tumor growth and contribute to tumor immune escape through the inhibition of T cell proliferation [95–97]. A recent study looking at 4T1 tumors demonstrated that IDO-1 expression was largely restricted to Gr-1+ myeloid vascular cells in the presence of IL-6 and IFNγ. IDO-1 expression has been demonstrated to regulate the neovascularization of tumors [98]. This is interesting because a study examining the impact of BP3 on tumor initiation noted elevated tumor vascularization following BP3 exposure [56]. Increased *Ido1* expression is also associated with tumor dormancy in some models [99]. It is tempting to speculate that the observed reduction in Ki-67 positive cells in the lung metastases of BP3 treated mice might be related to induction of tumor cell dormancy. Future studies will be required to determine the exact role of IDO-1 in BP3 treated 4T1 lung metastases.

One of the key immune cell types that are involved in cancer progression are T cells. CD4 T cells that receive signals from neighboring tumor cells often transition to a more Th2-like phenotype [100,101]. In turn, the Th2 cells secrete cytokines (i.e., IL4, IL5) that regulate B cell activity and allergic changes, while inhibiting Th1 polarization critical for cancer prevention [102,103]. Additionally, $CD4^+$ T cells can be polarized towards T regulatory cells (Tregs) in the presence of TGF-beta, which suppresses T cell activation/proliferation and facilitates immune escape leading to 4T1 lung metastases [57,61]. We observed a significant decline in the overall number of T cells in the animals exposed to 70 mg/kg BW/day BP3 consistent with an immune suppressive lung microenvironment, however, this included the Tregs as well. To examine the direct impact of BP3 on CD4 T lymphocytes, cell culture studies were performed under controlled conditions to examine activation-induced proliferation, cytokine production, and Treg polarization in the presence of TGF-β. Our cell culture data did not suggest a Th2 bias in cytokine production following activation, as we initially hypothesized. However, BP3 did suppress proliferation and cytokine secretion in general. While the T cells were able to polarize toward $Foxp3^+$ $CD25^+$ expressing cells, the phenotype appeared unstable. We suspect the presence of the lightly staining Foxp3+ cells in lung metastases of the animals that received 70 mg/kg BW/day BP3 is due to this instability. Interestingly, the impact of BP3 on Foxp3 was not a systemic effect. This suggests that in the lung metastases the effect of BP3 involved the contribution of both

the tissue and the tumor cells. It is well known that activation-induced T cell proliferation and cytokine production require IL2 signaling and metabolic changes (glycolysis) to drive the energy required for this activation [104]. Analysis of several glycolysis related gene transcripts demonstrated that BP3 did not impact the overall transcription of the glycolytic program, however the expression of lactate dehydrogenase A (*Ldha*) was significantly reduced following exposure to BP3. The LDHA enzyme is important for the conversion of lactate and pyruvate, and in $CD8^+$ T cells, as well as NK cells, LDHA is critical for cytotoxic activity [105,106]. Future research will determine the impact of BP3 on LDHA *in vivo* and its contribution to the tumor microenvironment.

Taken together, our results support an impact of BP3 on lung metastasis through an undefined mechanism that likely involves cross-talk between lung stroma cells and immune populations. Our observations of BP3 immunosuppression are consistent with previous research showing that exposures to estrogenic EDCs like BP3 can result in suppressed immune responses or immune toxicity [107–110]. The *in vivo* impact appears to be tissue dependent, as the decrease in T cell populations is only seen in the lung tumor metastases and the mammary lymph nodes. Here we have demonstrated that following exposure to 30 μM BP3 *in vitro*, proper T cell function is greatly inhibited. This work suggests that exposure to BP3 can facilitate growth of a triple negative breast cancer cell line in the lung and that this is associated with changes in the immune microenvironment. Future studies are required to understand the contribution of the specific cell populations and chemokine cascade, as well as whether there is a concern for women with TNBC following epidermal exposures to BP3.

Supplementary Material

Refer to Web version on PubMed Central for supplementary material.

Acknowledgments

The authors are grateful to Jennifer Ser-Dolansky and HistoSpring for help with immunohistochemical staining. We would like to thank Benjamin Covici, Ruth Estien Garcia, Le'naih DeJesus, Savanna Mason, Rooa Abdelmagid, and Renata Franca for their help with cell culture and image analysis. We would also like to thank the lab of Dr. Barbara Osborne for their help with immune cell cultures.

Funding

This study was supported in part by research grant from the National Institute of Environmental Health Sciences and the National Cancer Institute U01ES026140 (to DJJ and SSS) and U01ES026119 (to RS) and U01ES026137 (SC). Also, a supplement was awarded by the coordinating center at the University of Wisconsin U01 ES026127 (to SSS, SC, and RCS) to continue the studies with a focus on the immune impact.

Data availability

Data will be made available on request.

References

[1]. MacOn MB, Fenton SE, Endocrine disruptors and the breast: early life effects and later life disease, J. Mammary Gland Biol. Neoplasia 18 (2013) 43–61, 10.1007/s10911-013-9275-7. Preprint at. [PubMed: 23417729]

[2]. Yager JD, Davidson NE, Estrogen carcinogenesis in breast cancer, N. Engl. J. Med. 354 (2006) 270–282. [PubMed: 16421368]

[3]. Zhang HZ, Bennett JM, Smith KT, Sunil N, Haslam SZ, Estrogen mediates mammary epithelial cell proliferation in serum-free culture indirectly via mammary stroma-derived hepatocyte growth factor, Endocrinology 143 (2002) 3427–3434. [PubMed: 12193555]

[4]. Feng Y, Manka D, Wagner KU, Khan SA, Estrogen receptor-α expression in the mammary epithelium is required for ductal and alveolar morphogenesis in mice, Proc. Natl. Acad. Sci. U. S. A. 104 (2007), 14718. [PubMed: 17785410]

[5]. Knower KC, To SQ, Leung YK, Ho SM, Clyne CD, Endocrine disruption of the epigenome: a breast cancer link, Endocr. Relat. Cancer 21 (2014), 10.1530/ERC-13-0513. T33 Preprint at.

[6]. Thomas Zoeller R, et al. , Endocrine-disrupting chemicals and public health protection: a statement of principles from the Endocrine Society, Endocrinology 153 (2012) 4097–4110. [PubMed: 22733974]

[7]. la Merrill MA, et al. , Consensus on the key characteristics of endocrine-disrupting chemicals as a basis for hazard identification, Nat. Rev. Endocrinol. 16 (2019) 45–57, 2019 16:1. [PubMed: 31719706]

[8]. Garcia-Reyero N, The clandestine organs of the endocrine system, Gen. Comp. Endocrinol. 257 (2018) 264–271. [PubMed: 28822775]

[9]. Novel estrogenic action of the pesticide residue β-hexachlorocyclohexane in human breast cancer Cells1 | cancer research | American association for cancer research. https://aacrjournals.org/cancerres/article/56/23/5403/502822/Novel-Estrogenic-Action-of-the-Pesticide-Residue.

[10]. Lauby-Secretan B, et al. , Carcinogenicity of polychlorinated biphenyls and polybrominated biphenyls, Lancet Oncol. 14 (2013) 287–288. [PubMed: 23499544]

[11]. Katchy A, et al. , Coexposure to phytoestrogens and bisphenol a mimics estrogenic effects in an additive manner, Toxicol. Sci. 138 (2014) 21–35. [PubMed: 24284790]

[12]. Sengupta S, Obiorah I, Maximov PY, Curpan R, Jordan VC, Molecular mechanism of action of bisphenol and bisphenol A mediated by oestrogen receptor alpha in growth and apoptosis of breast cancer cells, Br. J. Pharmacol. 169 (2013) 167–178. [PubMed: 23373633]

[13]. Soto AM, Brisken C, Schaeberle C, Sonnenschein C, Does cancer start in the womb? Altered mammary gland development and predisposition to breast cancer due to in utero exposure to endocrine disruptors, J. Mammary Gland Biol. Neoplasia 18 (2013) 199. [PubMed: 23702822]

[14]. Matouskova K, Vandenberg LN, Towards a paradigm shift in environmental health decision-making: a case study of oxybenzone, Environ. Health 21 (2022) 1–12. [PubMed: 34980119]

[15]. Krause M, et al. , Sunscreens: are they beneficial for health? An overview of endocrine disrupting properties of UV-filters, Int. J. Androl. 35 (2012) 424–436, 10.1111/j.1365-2605.2012.01280.x. Preprint at. [PubMed: 22612478]

[16]. Kerdivel G, et al. , Estrogenic potency of benzophenone UV filters in breast cancer cells: proliferative and transcriptional activity substantiated by docking analysis, PLoS One 8 (2013).

[17]. Schlumpf M, et al. , In vitro and in vivo estrogenicity of UV screens, Environ. Health Perspect. 109 (2001) 239–244.

[18]. Journe F, Marguery MC, Rakotondrazafy J, El Sayed FE, Bazex J, Sunscreen sensitization: a 5-year study, Acta Derm. Venereol. 79 (1999) 211–213. [PubMed: 10384919]

[19]. Matta MK, et al. , Effect of sunscreen application under maximal use conditions on plasma concentration of sunscreen active ingredients: a randomized clinical trial, JAMA 321 (2019) 2082. [PubMed: 31058986]

[20]. Matouskova K, Vandenberg LN, UV screening chemicals, Reproductive and Developmental Toxicology (2022) 911–930, 10.1016/B978-0-323-89773-0.00045-X.

[21]. Philippat C, et al. , Prenatal exposure to environmental phenols: concentrations in amniotic fluid and variability in urinary concentrations during pregnancy, Environ. Health Perspect. 121 (2013) 1225–1231. [PubMed: 23942273]

[22]. DiNardo JC, Downs CA, Dermatological and environmental toxicological impact of the sunscreen ingredient oxybenzone/benzophenone-3, J. Cosmet. Dermatol. 17 (2018) 15–19. [PubMed: 29086472]

[23]. Schneider SL, Lim HW, Review of environmental effects of oxybenzone and other sunscreen active ingredients, J. Am. Acad. Dermatol. 80 (2019) 266–271, 10.1016/j.jaad.2018.06.033. Preprint at. [PubMed: 29981751]

[24]. Jones RJ, Testing the 'photoinhibition' model of coral bleaching using chemical inhibitors, Mar. Ecol. Prog. Ser. 284 (2004) 133–145.

[25]. Danovaro R, et al. , Sunscreens cause coral bleaching by promoting viral infections, Environ. Health Perspect. 116 (2008) 441–447. [PubMed: 18414624]

[26]. Matouskova K, Jerry D, Toxicology LV-R, Undefined. Exposure to Low Doses of Oxybenzone during Perinatal Development Alters Mammary Gland Morphology in Male and Female Mice, Elsevier, 2020.

[27]. LaPlante CD, Bansal R, Dunphy KA, Jerry DJ, Vandenberg LN, Oxybenzone alters mammary gland morphology in mice exposed during pregnancy and lactation, J Endocr Soc 2 (2018) 903–921. [PubMed: 30057971]

[28]. Coronado M, et al. , Estrogenic activity and reproductive effects of the UV-filter oxybenzone (2-hydroxy-4-methoxyphenyl-methanone) in fish, Aquat. Toxicol. 90 (2008) 182–187. [PubMed: 18930325]

[29]. Kim S, Kim S, Won S, Choi K, Considering common sources of exposure in association studies - urinary benzophenone-3 and DEHP metabolites are associated with altered thyroid hormone balance in the NHANES 2007–2008, Environ. Int. 107 (2017) 25–32. [PubMed: 28651165]

[30]. Aker AM, et al. , Associations between maternal phenol and paraben urinary biomarkers and maternal hormones during pregnancy: a repeated measures study, Environ. Int. 113 (2018) 341–349. [PubMed: 29366524]

[31]. Janjua NR, et al. , Systemic absorption of the sunscreens benzophenone-3, octyl-methoxycinnamate, and 3-(4-methyl-benzylidene) camphor after whole-body topical application and reproductive hormone levels in humans, J. Invest. Dermatol. 123 (2004) 57–61. [PubMed: 15191542]

[32]. Scinicariello F, Buser MC, Serum testosterone concentrations and urinary bisphenol A, benzophenone-3, triclosan, and paraben levels in male and female children and adolescents: nhanes 2011–2012, Environ. Health Perspect. 124 (2016) 1898–1904. [PubMed: 27383665]

[33]. Schlumpf M, et al. , In vitro and in vivo estrogenicity of UV screens, Environ. Health Perspect. 109 (2001) 239–244.

[34]. Williams GP, Darbre PD, Low-dose environmental endocrine disruptors, increase aromatase activity, estradiol biosynthesis and cell proliferation in human breast cells, Mol. Cell. Endocrinol. 486 (2019) 55–64. [PubMed: 30817981]

[35]. Phiel KL, Henderson RA, Adelman SJ, Elloso MM, Differential estrogen receptor gene expression in human peripheral blood mononuclear cell populations, Immunol. Lett. 97 (2005) 107–113. [PubMed: 15626482]

[36]. Abbas AK, Murphy KM, Sher A, Functional diversity of helper T lymphocytes, Nature 383 (1996) 787–793. [PubMed: 8893001]

[37]. Singh V, Agrewala JN, Regulatory role of pro-Th1 and pro-Th2 cytokines in modulating the activity of Th1 and Th2 cells when B cell and macrophages are used as antigen presenting cells, BMC Immunol. 7 (2006) 1–10. [PubMed: 16405726]

[38]. Panina-Bordignon P, et al. , The C-C chemokine receptors CCR4 and CCR8 identify airway T cells of allergen-challenged atopic asthmatics, J. Clin. Invest. 107 (2001) 1357–1364. [PubMed: 11390417]

[39]. Balashov KE, Rottman JB, Weiner HL, Hancock WW, CCR5 and CXCR3 T Cells Are Increased in Multiple Sclerosis and Their Ligands MIP-1 and IP-10 Are Expressed in Demyelinating Brain Lesions, 96, 1999, pp. 6873–6878.

[40]. Olive AJ, Gondek DC, Starnbach MN, CXCR3 and CCR5 are both required for T cell mediated protection against C. TRACHOMATIS infection in the murine genital mucosa, Mucosal Immunol. 4 (2011) 208. [PubMed: 20844481]

[41]. Gu-Trantien C, et al. , CD4+ follicular helper T cell infiltration predicts breast cancer survival, J. Clin. Invest. 123 (2013) 2873. [PubMed: 23778140]

[42]. Varn FS, Mullins DW, Arias-Pulido H, Fiering S, Cheng C, Adaptive immunity programmes in breast cancer, Immunology 150 (2017) 25. [PubMed: 27564847]

[43]. Priyanka HP, Krishnan HC, Singh V, Hima L, Thyagarajan S, Estrogen modulates in vitro T cell responses in a concentration-and receptor-dependent manner: effects on intracellular molecular targets and antioxidant enzymes, Mol. Immunol. 56 (2013) 328–339. [PubMed: 23911387]

[44]. Karpuzoglu-Sahin E, Zhi-Jun Y, Lengi A, Sriranganathan N, Ahmed SA, EFFECTS of LONG-TERM estrogen treatment ON IFN-gamma, IL-2 and IL-4 gene expression and protein synthesis, in: SPLEEN AND THYMUS OF NORMAL C57BL/6 MICE, 2001, 10.1006/cyto.2001.0876.

[45]. Polanczyk MJ, et al. , Cutting edge: estrogen drives expansion of the CD4+CD25 + regulatory T cell compartment, J. Immunol. 173 (2004) 2227–2230. [PubMed: 15294932]

[46]. Offner H, Adlard K, Zamora A, Vandenbark AA, Estrogen potentiates treatment with T-cell receptor protein of female mice with experimental encephalomyelitis, J. Clin. Invest. 105 (2000) 1465–1472. [PubMed: 10811854]

[47]. Tai P, et al. , Induction of regulatory T cells by physiological level estrogen, J. Cell. Physiol. 214 (2008) 456–464. [PubMed: 17654501]

[48]. Gregory KJ, Morin SM, Schneider SS, Regulation of early growth response 2 expression by secreted frizzled related protein 1, BMC Cancer 17 (2017) 473. [PubMed: 28687085]

[49]. Duffy JP, Smith PJ, Crocker J, Matthews HR, Combined staining method for the demonstration of tissue eosinophils and mast cells, J. Histotechnol. 16 (1993) 143–144.

[50]. Wong KE, et al. , Evaluation of Rhodiola Crenulata on Growth and Metabolism of NB-1691, an MYCN-Amplified Neuroblastoma Cell Line, 2018, 10.1177/1010428318779515.

[51]. Gauger KJ, Hugh JM, Troester MA, Schneider SS, Down-regulation of sfrp1 in a mammary epithelial cell line promotes the development of a cd44high/cd24low population which is invasive and resistant to anoikis, Cancer Cell Int. 9 (2009) 11. [PubMed: 19422694]

[52]. Gregory KJ, et al. , The relationship between the calcium-sensing receptor and secreted frizzled related protein in the breast, Journal of Molecular Oncology Research 2 (2018).

[53]. Ozay EI, et al. , Cell-penetrating anti-protein kinase C theta antibodies act intracellularly to generate stable, highly suppressive regulatory T cells, Mol. Ther. 28 (2020) 1987. [PubMed: 32492367]

[54]. Anadón A, et al. , Toxicological evaluation of benzophenone, EFSA J. 7 (2009) 1104.

[55]. Gonzalez H, Farbrot A, Larkö O, Wennberg AM, Percutaneous absorption of the sunscreen benzophenone-3 after repeated whole-body applications, with and without ultraviolet irradiation, Br. J. Dermatol. 154 (2006) 337–340. [PubMed: 16433806]

[56]. Kariagina A, et al. , Benzophenone-3 promotion of mammary tumorigenesis is diet-dependent, Oncotarget 11 (2020) 4465. [PubMed: 33400736]

[57]. Olkhanud PB, et al. , Breast cancer lung metastasis requires expression of chemokine receptor CCR4 and T regulatory cells, Cancer Res. 69 (2009) 5996. [PubMed: 19567680]

[58]. Vadrevu SK, et al. , Studying the role of alveolar macrophages in breast cancer metastasis, JoVE 2016 (2016), 54306.

[59]. Kwiecień I, et al. , CD163 and CCR7 as markers for macrophage polarization in lung cancer microenvironment, Cent. Eur. J. Immunol. 44 (2019) 395.

[60]. Steenbrugge J, et al. , Comparative profiling of metastatic 4T1- vs. Non-metastatic py230-based mammary tumors in an intraductal model for triple-negative breast cancer, Front. Immunol. 10 (2019) 2928. [PubMed: 31921184]

[61]. Olkhanud PB, et al. , Tumor-evoked regulatory B cells promote breast cancer metastasis by converting resting CD4+ T cells to T regulatory cells, Cancer Res. 71 (2011) 3505. [PubMed: 21444674]

[62]. Mandal PK, et al. , CCL2 conditionally determines CCL22-dependent Th2-accumulation during TGF-β-induced breast cancer progression, Immunobiology 223 (2018) 151–161. [PubMed: 29107385]

[63]. Wei S, Kryczek I, Blood WZ, Undefined. Regulatory T-Cell Compartmentalization and Trafficking, 2006 (ashpublications.org).

[64]. Gobert M, et al. , Regulatory T cells recruited through CCL22/CCR4 are selectively activated in lymphoid infiltrates surrounding primary breast tumors and lead to an adverse clinical outcome, Cancer Res. 69 (2009) 2000–2009. [PubMed: 19244125]

[65]. Staudt LM, Dent AL, Shaffer AL, Yu X, Regulation of lymphocyte cell fate decisions and lymphomagenesis by BCL-6, Int. Rev. Immunol. 18 (1999) 381–403. [PubMed: 10626250]

[66]. Zheng WP, Flavell RA, The transcription factor GATA-3 is necessary and sufficient for Th2 cytokine gene expression in CD4 T cells, Cell 89 (1997) 587–596. [PubMed: 9160750]

[67]. Szabo SJ, et al. , A novel transcription factor, T-bet, directs Th1 lineage commitment, Cell 100 (2000) 655–669. [PubMed: 10761931]

[68]. Delgoffe GM, et al. , Stability and function of regulatory T cells is maintained by a neuropilin-1-semaphorin-4a axis, Nature 501 (2013) 252–256. [PubMed: 23913274]

[69]. Nakagawa Y, interactions TS-C, Undefined. Metabolism of 2-Hydroxy-4-Methoxybenzophenone in Isolated Rat Hepatocytes and Xenoestrogenic Effects of its Metabolites on MCF-7 Human Breast Cancer, Elsevier, 2002.

[70]. Fö C et al. Involvement of Estrogen Receptor β in Terminal Differentiation of Mammary Gland Epithelium. National Acad Sciences.

[71]. Schlumpf M, et al. , In vitro and in vivo estrogenicity of UV screens, Environ. Health Perspect. 109 (2001) 239–244.

[72]. Rooney J, et al. , A gene expression biomarker identifies chemical modulators of estrogen receptor α in an MCF-7 microarray compendium, ACS Publications 34 (2021) 313–329.

[73]. Dent R, et al. , Triple-negative breast cancer: clinical features and patterns of recurrence, Clin. Cancer Res. 13 (2007) 4429–4434. [PubMed: 17671126]

[74]. Takai K, Le A, Weaver VM, Werb Z, Targeting the cancer-associated fibroblasts as a treatment in triple-negative breast cancer, Oncotarget 7 (2016) 82889–82901. [PubMed: 27756881]

[75]. Steenbrugge J, et al. , Anti-inflammatory signaling by mammary tumor cells mediates prometastatic macrophage polarization in an innovative intraductal mouse model for triple-negative breast cancer, J. Exp. Clin. Cancer Res. 37 (2018).

[76]. Chen D, Mellman I, Elements of cancer immunity and the cancer–immune set point, Nature 541 (7637) (2017) 321–330. [PubMed: 28102259]

[77]. Hanahan D, cell LC-C, Undefined. Accessories to the Crime: Functions of Cells Recruited to the Tumor Microenvironment, Elsevier, 2012.

[78]. Madera L, Greenshields A, Coombs MRP, Hoskin DW, 4T1 murine mammary carcinoma cells enhance macrophage-mediated innate inflammatory responses, PLoS One 10 (2015), e0133385. [PubMed: 26177198]

[79]. Ouzounova M, et al. , Monocytic and granulocytic myeloid derived suppressor cells differentially regulate spatiotemporal tumour plasticity during metastatic cascade, Nat. Commun. 8 (2017).

[80]. Hughes E, et al. , Primary breast tumours but not lung metastases induce protective anti-tumour immune responses after Treg-depletion, Cancer Immunol. Immunother. 69 (2020) 2063–2073. [PubMed: 32447412]

[81]. DuPré SA, Redelman D, Hunter KW, The mouse mammary carcinoma 4T1: characterization of the cellular landscape of primary tumours and metastatic tumour foci, Int. J. Exp. Pathol. 88 (2007) 351. [PubMed: 17877537]

[82]. Olkhanud PB, et al. , Breast cancer lung metastasis requires expression of chemokine receptor CCR4 and T regulatory cells, Cancer Res. 69 (2009) 5996. [PubMed: 19567680]

[83]. Rego SL, Helms RS, Dréau D, Breast tumor cell TACE-shed MCSF promotes pro-angiogenic macrophages through NF-κB signaling, Angiogenesis 17 (2014) 573–585. [PubMed: 24197832]

[84]. Yoshimura T, et al. , Monocyte chemoattractant protein-1/CCL2 produced by stromal cells promotes lung metastasis of 4T1 murine breast cancer cells, PLoS One 8 (2013), 58791.

[85]. Jin J, et al. , CCL2: an important mediator between tumor cells and host cells in tumor microenvironment, Front. Oncol. 11 (2021) 2917.

[86]. Han B, et al. , A chemokine regulatory loop induces cholesterol synthesis in lung-colonizing triple-negative breast cancer cells to fuel metastatic growth, Mol. Ther. 30 (2022) 672–687. [PubMed: 34274535]

[87]. Tsuyada A, et al. , CCL2 mediates cross-talk between cancer cells and stromal fibroblasts that regulates breast cancer stem cells, Cancer Res. 72 (2012) 2768–2779. [PubMed: 22472119]

[88]. Kitamura T, et al. , CCL2-induced chemokine cascade promotes breast cancer metastasis by enhancing retention of metastasis-associated macrophages, J. Exp. Med. 212 (2015) 1043–1059. [PubMed: 26056232]

[89]. Luo A, et al. , Myeloid-derived suppressor cells recruited by chemokine (C-C motif) ligand 3 promote the progression of breast cancer via phosphoinositide 3-kinase-protein kinase B-mammalian target of rapamycin signaling, J Breast Cancer 23 (2020) 141–161. [PubMed: 32395374]

[90]. Penido C, et al. , LPS induces eosinophil migration via CCR3 signaling through a mechanism independent of RANTES and eotaxin, Am. J. Respir. Cell Mol. Biol. 25 (2001). www.atsjournals.org.

[91]. Rot A, et al. , RANTES and macrophage inflammatory protein 1 alpha induce the migration and activation of normal human eosinophil granulocytes, J. Exp. Med. 176 (1992) 1489–1495. [PubMed: 1281207]

[92]. Yi S, et al. , Eosinophil recruitment is dynamically regulated by interplay among lung dendritic cell subsets after allergen challenge, Nat. Commun. 9 (2018) 1–14, 2018 9:1. [PubMed: 29317637]

[93]. Pinho V, et al. , The role of CCL22 (MDC) for the recruitment of eosinophils during allergic pleurisy in mice, J. Leukoc. Biol. 73 (2003) 356–362. [PubMed: 12629149]

[94]. Driesen J, Popov A, Schultze JL, CD25 as an immune regulatory molecule expressed on myeloid dendritic cells, Immunobiology 213 (2008) 849–858. [PubMed: 18926299]

[95]. Frumento G, et al. , Tryptophan-derived catabolites are responsible for inhibition of T and natural killer cell proliferation induced by indoleamine 2,3-dioxygenase, J. Exp. Med. 196 (2002) 459–468. [PubMed: 12186838]

[96]. Rad Pour S, et al. , Exhaustion of CD4+ T-cells mediated by the kynurenine pathway in melanoma, Sci. Rep. 9 (2019) 1–11, 2019 9:1. [PubMed: 30626917]

[97]. Bishnupuri KS, et al. , IDO1 and kynurenine pathway metabolites activate PI3K-akt signaling in the neoplastic colon epithelium to promote cancer cell proliferation and inhibit apoptosis, Cancer Res. 79 (2019) 1138–1150. [PubMed: 30679179]

[98]. Dey S, et al. , IDO1 signaling through GCN2 in a subpopulation of Gr-1þ cells shifts the IFNg/IL6 balance to promote neovascularization, Cancer Immunol Res 9 (2021) 514–528. [PubMed: 33622713]

[99]. Lopes-Bastos B, et al. , Association of breast carcinoma growth with a non-canonical axis of IFNγ/IDO1/TSP1, Oncotarget 8 (2017) 85024–85039. [PubMed: 29156701]

[100]. Zhu X, Du L, Feng J, Ling Y, Xu S, Clinicopathological and prognostic significance of serum cytokine levels in breast cancer, Clin. Lab. 7 (2014) 1145–1151.

[101]. Slaney CY, Kershaw MH, Darcy PK, Trafficking of T cells into tumors, Cancer Res. 74 (2014) 7168–7174. [PubMed: 25477332]

[102]. Wurtz O, Bajénoff M, Guerder S, IL-4-mediated inhibition of IFN-γ production by CD4+ T cells proceeds by several developmentally regulated mechanisms, Int. Immunol. 16 (2004) 501–508. [PubMed: 14978023]

[103]. Gu Y, et al. , Interleukin 10 suppresses Th17 cytokines secreted by macrophages and T cells, Eur. J. Immunol. 38 (2008) 1807–1813. [PubMed: 18506885]

[104]. Malek TR, et al. , IL-2 family of cytokines in T regulatory cell development and homeostasis, J. Clin. Immunol. 28 (2008) 635–639. [PubMed: 18726679]

[105]. Sheppard S, et al. , Lactate dehydrogenase A-dependent aerobic glycolysis promotes natural killer cell anti-viral and anti-tumor function, Cell Rep. 35 (2021).

[106]. Xu K, et al. , Glycolysis fuels phosphoinositide 3-kinase signaling to bolster T cell immunity, Science 371 (2021) 405–410. [PubMed: 33479154]

[107]. Robinson L, Miller R, The impact of bisphenol A and phthalates on allergy, asthma, and immune function: a review of latest findings, Curr Environ Health Rep 2 (2015) 379–387. [PubMed: 26337065]

[108]. Kuo C, Yang S, Kuo P, Undefined. Immunomodulatory Effects of Environmental Endocrine Disrupting Chemicals, Elsevier, 2012 medical, C. H.-T. K. journal of.

[109]. Chalubinski M, Allergy MK, Undefined. Endocrine Disrupters–Potential Modulators of the Immune System and Allergic Response, 61, Wiley Online Library, 2006, pp. 1326–1335, 2006.

[110]. Toxicology SA, Undefined. The Immune System as a Potential Target for Environmental Estrogens (Endocrine Disrupters): a New Emerging Field, Elsevier, 2000.

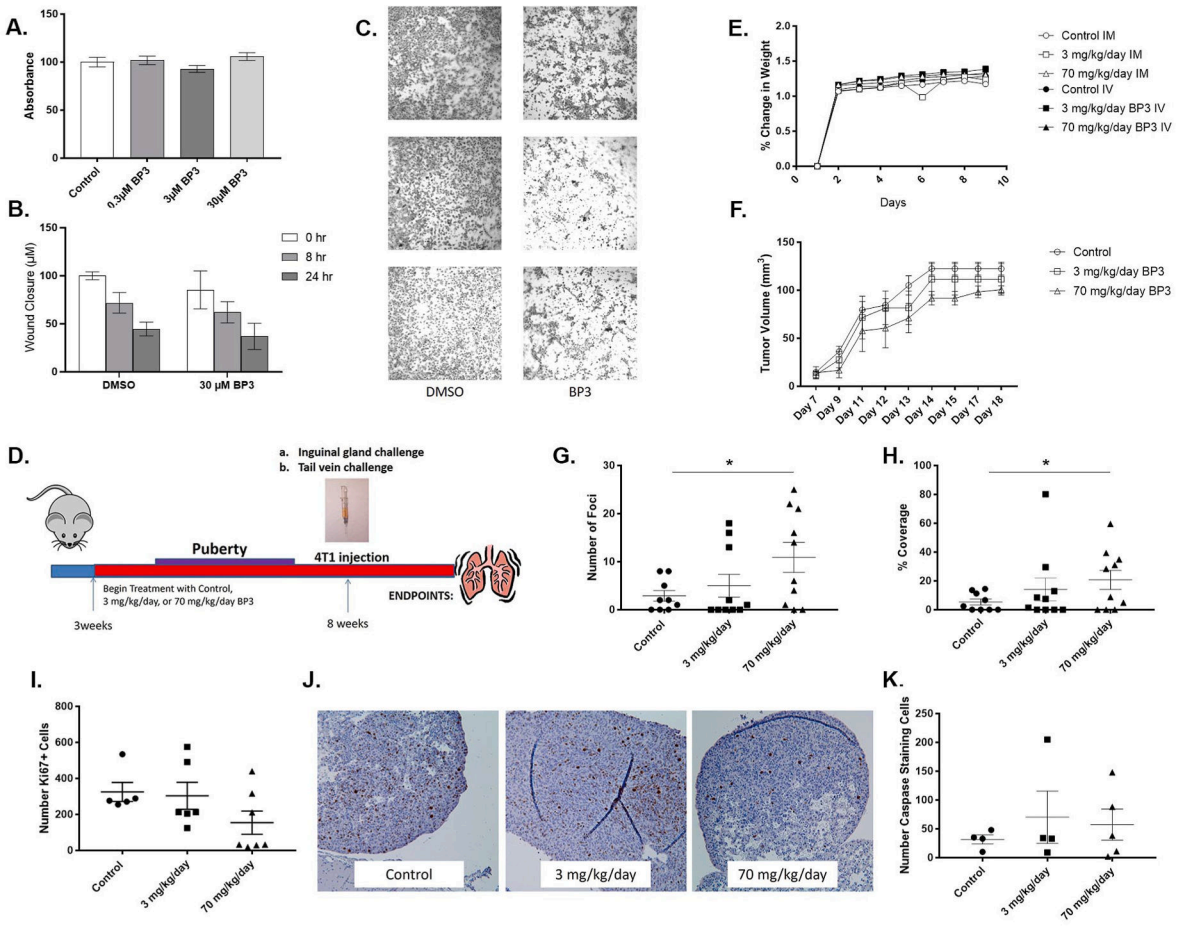

Fig. 1. BP3 induces 4T1 proliferation in vivo.

4T1s were treated directly with 30 μM BP3 and **A.** proliferation of 4T1 cancer cells was measured via MTS assay. Migration of the 4T1s was measured through **B.** scratch wound assay and **C.** transwell migration assay. **D.** Schematic of Balb/c mouse experiment. **E.** Tumor volume in mice injected with 4T1 in the mammary fat pad starting on day 7 post injection using the formula V = (W (2) * L)/2 where V is volume, W is tumor width, and L is length. **F.** Mice were weighed throughout the experiment, and the change in weight was calculated starting at time of injection. **G.** Tumor foci in IV lung sections from IV mice were counted upon staining with H&E. **H.** In the IV lung H&E sections, the percent tumor coverage was calculated via measurement of total tumor size divided by total lung area. **I.** IV lung sections were stained with Ki67, and the total number of positive cells in the metastasis were counted. **J.** Representative images of Ki67 staining in IV lung tumor metastases. **K.** IV lungs were stained with cleaved caspase 3 and total number of positive cells were counted in the metastases.

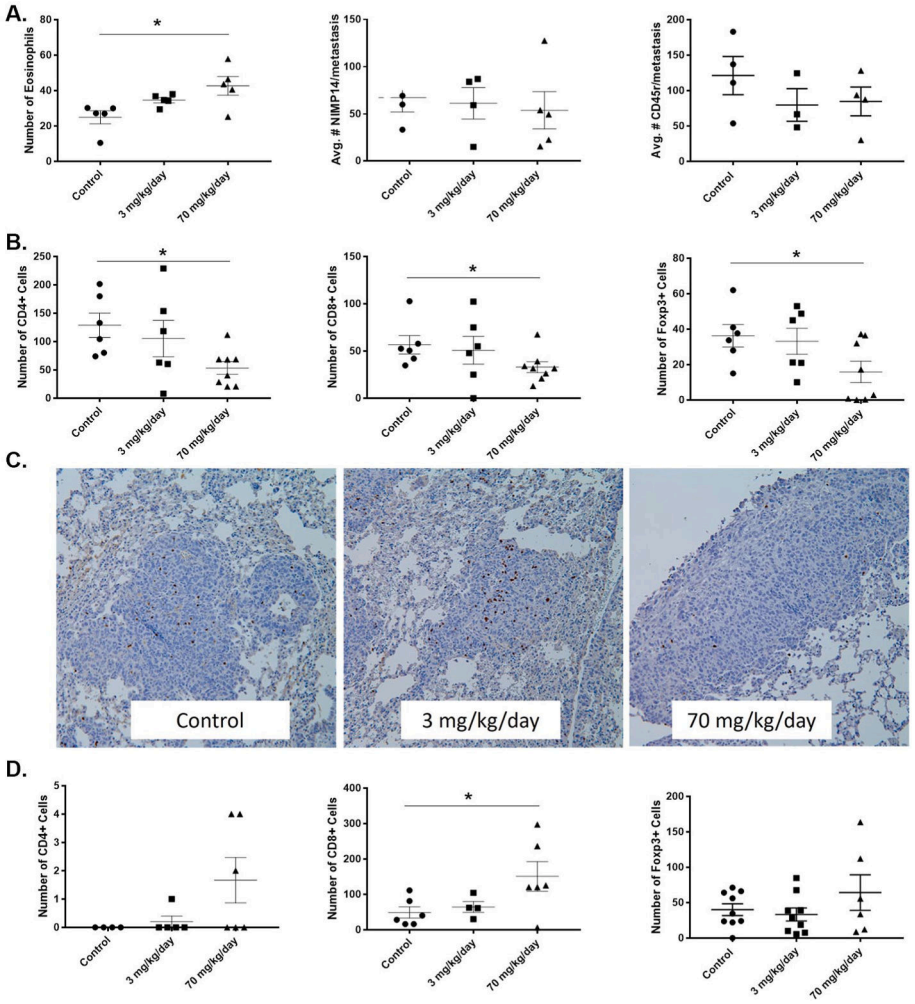

Fig. 2. BP3 alters immune populations in a tissue specific manner.

A. Immunohistochemistry was performed on lungs from IV mice that were paraffine embedded, to observe immune populations. From left to right, Vital New Red for eosinophils, Nimp-14 for neutrophils, CD45r for B cells. Positively staining cells were counted in the metastases of the lung. **B.** Lungs from IV mice were stained with T cell markers (left to right) T helper cells, cytotoxic T cells, and Tregs. **C.** Representative images from the lung metastasis of the IV group staining with Foxp3. **D.** Tumor from IM mice were paraffin embedded, sectioned and stained for T cell markers.

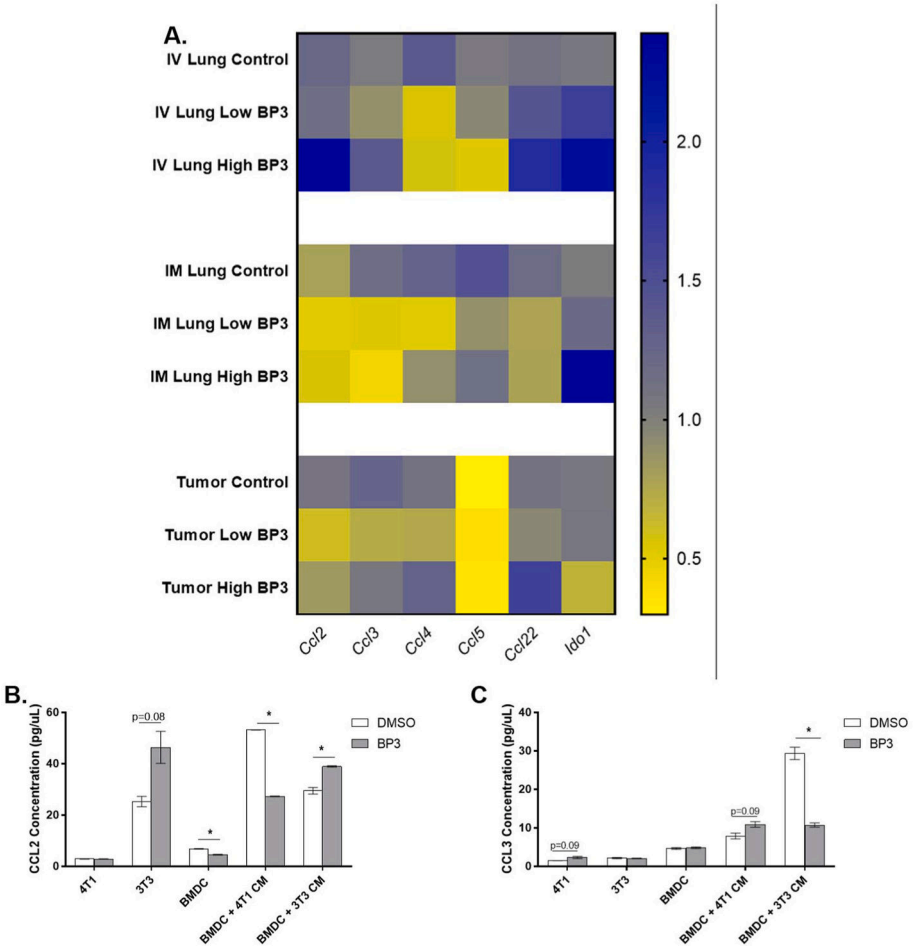

Fig. 3. BP3 alters cytokine expression

A. RNA was harvested from sections of whole tissue from both IM and IV mice exposed to BP3. mRNA levels of the various cytokines were analyzed by qRT-PCR. All qRT-PCR results were performed with n = 5 and results were normalized to *ATCB.* **B, C.** Cells were exposed to 30 μM BP3 *in vitro* or exposed to conditioned media from cells that were exposed to BP3. Supernatant was collected and protein levels of CCL2 or CCL3 were measured via ELISA.

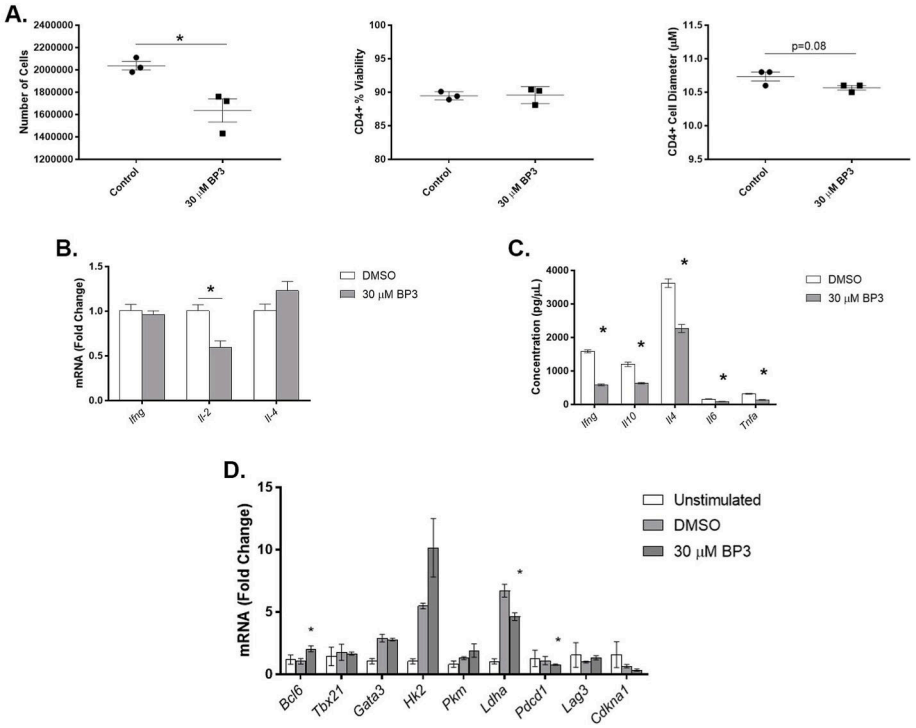

Fig. 4. ***BP3 alters T cell expansion and cytokine expression*** **in vitro**

T cells were harvested from spleens of female 5-week Balb/c mice and activated via the presence of plate-bound CD3, CD28, and IL-2 in the media. **A.** Cell number, % viability, and cell diameter were quantified using the ChemoMetec NucleoCounter Nc-202. **B.** Gene expression of T cell activation genes was measured via qRT-PCR. All qRT = PCR reactions were run in biological triplicate and technical duplicate. **C.** T cell related cytokines were measured from the media of activated T cells exposed to 30 μM BP3 through the use of MSD. **D.** T cell activation, senescence, and exhaustion gene expression markers were interrogated through the use of qRT-PCR.

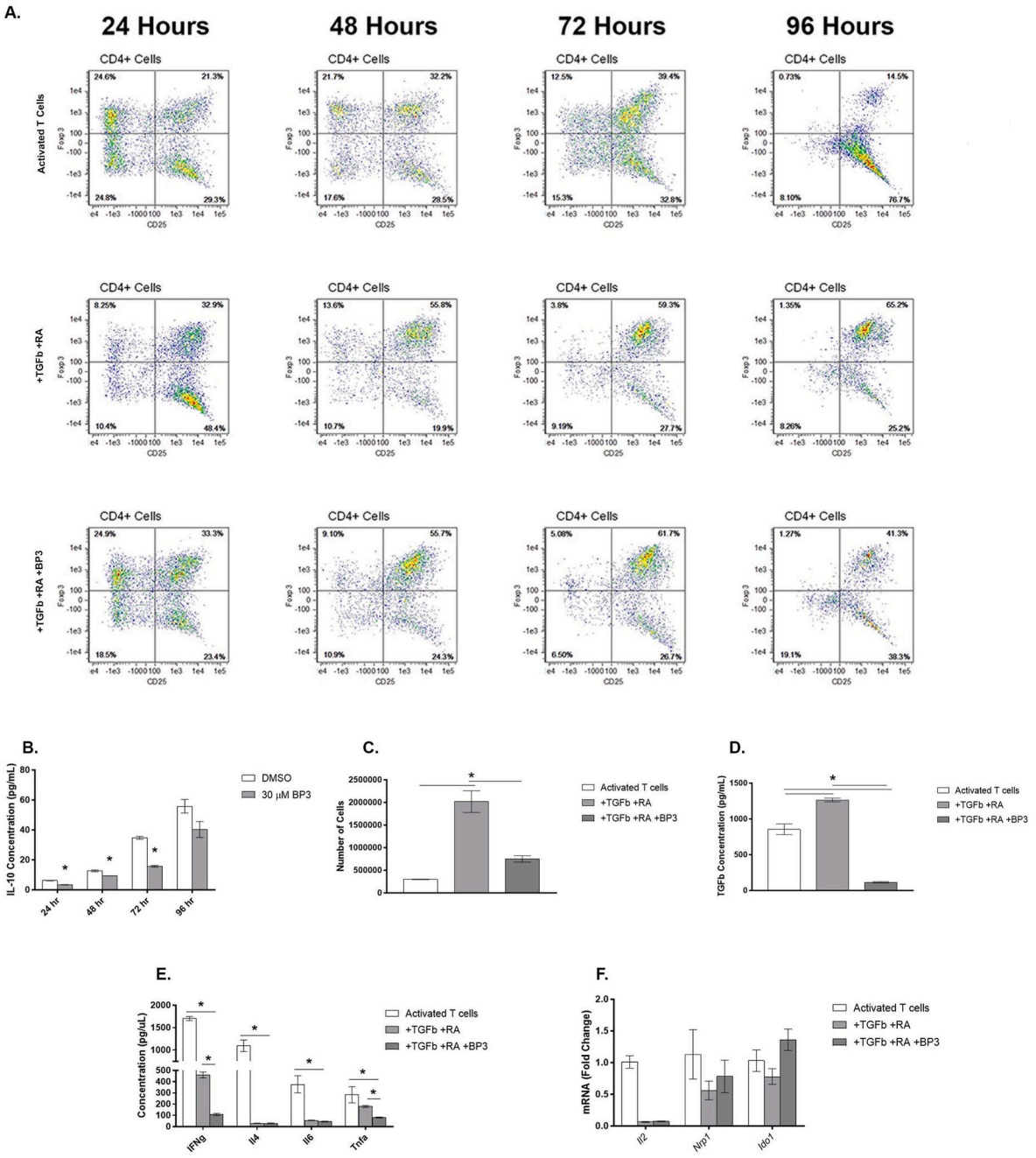

Fig. 5. Exposure to BP3 reduces the normal activity of T regulatory cells

T cells were activated and then polarized or not to the Tregs through the addition of TGFb and retinoic acid. **A.** Cell expression of the surface markers, CD4 and CD25, and the transcription factor, Foxp3 were measured by flow cytometry. **B.** Supernatant from the Tregs in A. was taken to measure secreted levels of Il-10 protein. **C.** Activated T cells or Tregs±BP3 were counted using the ChemoMetec NucleoCounter Nc-202. **D, E.** Supernatant from activated T cells or Tregs±BP3 was taken to measure secreted protein levels. **F.** RNA was isolated from activated T cells or Tregs±BP3 and gene expression of Treg associated

genes was measured through qRT-PCR, all reactions were measured in biological triplicate, technical duplicate.

Table 1

Immunohistochemistry antibodies.

Antibody	Vendor	Catalog #	Antibody Type/ Clone	Final dilution IHC	Antigen Retrieval	Detection system
Anti-CD45R (B220)	eBioscience Affymetrix	14–0452	Rat Monoclonal	1:200	Citrate buffer (pH6) 20 min	Dako polymer
Anti-NIMP-R14	Santa Cruz	sc-59338	Rat Monoclonal	1:50	Citrate buffer (pH6) 10 min	Dako polymer
Anti-CD8a	eBioscience Affymetrix	14–0808	Rat Monoclonal	1:100	Citrate buffer (pH6) 20 min	Dako polymer
Anti-CD4	eBioscience Affymetrix	14–9766	Rat Monoclonal	1:100	Citrate buffer (pH6) 20 min	Dako polymer
Anti-Foxp3	eBioscience Affymetrix	14–5773	Rat (JFK-16s)	1:100	Citrate buffer (pH6) 20 min	BD pharmgen rat/strep HRP
Anti-Mannose receptor (CD206)	Abcam	ab64693	Rabbit Polyclonal	1:200	Citrate buffer (pH6) 20 min	Dako polymer
Anti-CD163 [EPR19518]	Abcam	ab182422	Rabbit Monoclonal	1:200	Tris-EDTA (pH9) 20 min	Dako polymer
Anti-F4/80	Bio-Rad	MCA497R	Rat Monoclonal	1:100	Citrate buffer (pH6) 20 min	Dako polymer

Table 2

qRT-PCR Primers.

Gene	Forward	Reverse
Actb	*5′ CTA AGG CCA ACC GTG AAA AG 3′*	*5′ ACC AGA GGC ATA CAG GGA CA 3′*
Ccl2	*5′ CTG GAG AGC TAC AAG AGG AT 3′*	*5′ TGA GCT TGG TGA CAA AAA 3′*
Ccl3	*5′ TCT GCG CTG ACT CCA AAG AG 3′*	*5′ GTG GCT ACT TGG CAG CAA AC 3′*
Ccl4	*5′ CTG TGC AAA CCT AAC CCC GA 3′*	*5′ AGG GTC AGA GCC CAT TGG T 3′*
Ccl5	*5′ CAG TCG TGT TTG TCA CTC GAA 3′*	*5′ CCA TTT TCC CAG GAC CGA G 3′*
Ccl22	*5′ ACC TCT GAT GCA GGT CCC TAT 3′*	*5′ CTC ACA GAG TGA CAG CCC AG 3′*
Ido1	*5′ CGT GCC TGG TTT TGA GGT TT 3′*	*5′ GGT CCA CAA AGT CAC GCA TA 3′*
Helios	*5′ TGA CCC ACC TGT AAA GTG CT 3′*	*5′ CTT CCA TAG GCG GTA CAT GGT 3′*
Nrp1	*5′ CTC TCC TTC CCG CAG ACA AC 3′*	*5′ AAC ATT CGG GCC CTC TCT TG 3′*
Pmk	*5′ ATG CAG CAC CTG ATA GCT CG 3′*	*5′ AGG TCT GTG GAG TGA CTG GA 3′*
Hk2	*5′ GTT TCT CTA TTT GGC CCC GAC 3′*	*5′ AGA GAT ACT GGT CAA CCT TCT GC 3′*
Il2ra	*5′ TGG CAA CAC AGA TGG AGG A 3′*	*5′ TGG CGT CTC AGA TTT GGC TT 3′*
Gata3	*5′ AGT ACA GCT CTG GAC TCT TC 3′*	*5′ CTG CCT TCT GTG CTG GAT 3′*
Cdkn1a	*5′ GAT CCA CAG CGA TAT CCA GA 3′*	*5′ AAG TCA AAG TTC CAC CGT TC 3′*
Il4	*5′ TGT ACC AGG AGC CAT ATC CA 3′*	*5′ CTG TGG TGT TCT TCG TTG CT 3′*
Il2	*5′ TTG AGT GCC AAT TCG ATG AT 3′*	*5′ TTG AGG GCT TGT TGA GAT GA 3′*
Ifng	*5′ CCT TTG GAC CCT CTG ACT T 3′*	*5′ GTA ACA GCC AGA AAC AGC CA 3′*
Il10	*5′ TGA ATT CCC TGG GTG AGA AGC TGA 3′*	*5′ TGG CCT TGT AGA CAC CTT CCT CTT 3′*